Contrib Mineral Petrol (1995) 122:241–251

C. Ballhaus · C.G. Ryan

Platinum-group elements in the Merensky reef. I. PGE in solid solution in base metal sulfides and the down-temperature equilibration history of Merensky ores

Received: 25 April 1995/Accepted: 5 September 1995

Abstract The platinum-group elements (PGE) in base metal sulfides (BMS) of the Merensky reef are mostly close to the detection limit of the proton microprobe. The only phase that accommodates appreciable PGE is pentlandite. Total average PGE plus Au grades of the sulfide fraction of the Merensky reef are about 500 ppm. We estimate the modal proportions of the major BMS to be around 53 percent pyrrhotite, 25 percent pentlandite, and 22 percent chalcopyrite (ignoring minor phases). Using this estimate, we calculate by how much the sulfides are oversaturated with respect to individual PGE. With respect to Pt, the sulfides are many times oversaturated, i.e., nearly all Pt occurs as discrete PGE phases. With regard to Pd the sulfides are oversaturated by about a factor of two. The Ru and Rh levels are at and below saturation levels. Available experiments suggest that the entire PGE content of the sulfide fraction can easily be accommodated in solid solution in BMS at temperatures as low as 500°C. The fact that the BMS are oversaturated with most PGE thus indicates that the sulfides have continued to exsolve PGE below that temperature. Calculated sulfur fugacities indicate that f_{S_2} is controlled by silica activity, as expected in high-temperature ores, suggesting that metal/sulfur ratios of the ore may not have changed much since complete solidification of the intercumulus silicate melt of the Merensky reef. All sulfides investigated have cooled below the maximum temperature of pentlandite-pyrite coexistence, which experiments place at 250 ± 30°C. Final closure temperatures of the sulfide-PGE mineral assemblages, approximated by extrapolating the pentlandite-pyrrhotite solvus beyond its experimentally determined range, are possibly as low as 80 to 90°C.

C. Ballhaus (✉)[1]
Max-Planck-Institut für Chemie, Abteilung Kosmochemie, Saarstrasse 23, D-55122 Mainz, Germany

C. Ballhaus
Institut für Mineralogie, Universität Freiburg, Albertstrasse 23b, D-79104 Freiburg, Germany

C.G. Ryan
CSIRO Division Exploration and Mining, Dehli Road, North Ryde NSW 2113, Australia

[1] *Present address:* Geology Department, Australian National University, Canberra, ACT 0200, Australia

Editorial responsibility: V. Trommsdorff

Introduction

The average reported ore grades of the Merensky reef in the Bushveld Complex are ~ 8 ppm combined platinum-group elements (PGE) and Au, collectively referred to as noble metals (Naldrett et al. 1987). The sulfide fraction of the mineralized zone is rather small compared with other magmatic sulfide deposits, and only around 1.5 volume percent. If one recalculates all noble metals to 100 percent sulfide, the noble metal "tenor" of the sulfide fraction is ~ 500 ppm (Naldrett et al. 1986, 1987). Relative to the PGE and Au abundances in the presumed parent magma to the Merensky ore (Davies and Tredoux 1985) and other low-pressure melts (Ballhaus 1995), this requires enrichment factors from > 7000 for Au to > 20000 for Ir (Table 1) – easily the highest enrichment factors of any ore-forming process.

Recalculation of the noble metal abundances to 100 percent sulfide implies that the PGE and Au were brought into the ore horizon by a magmatic monosulfide liquid solution (mls). There is indeed evidence for the addition of a new magma at the level of what later became the Merensky reef, that may have supplied the PGE and/or the sulfur (Davies and Tredoux 1985; Lee and Tredoux 1986; for a summary see Naldrett et al. 1987); such as (1) discontinuities in the $^{87}Sr/^{86}Sr$ isotope profiles across the ore zone (Kruger and Marsh 1982); (2) reversals in the Mg/(Mg + Fe) and Ca/(Ca + Na) ratios in cumulus pyroxene and plagioclase (Naldrett et al. 1986; Ballhaus et al. 1988); and (3)

Table 1 PGE enrichment in Merensky ore. References: (1) PGE abundance calculated in ppm in 100 percent sulfide, from Naldrett et al. (1987); (2) PGE abundance in ppb from Davies and Tredoux (1985); (3) Nernst sulfide/silicate partition coefficients determined by Peach et al. (1990); (4) Ir, Pt, Pd and Au Nernst sulfide/silicate partition coefficients from Stone et al. (1990), Ru and Rh coefficients from Bezmen et al. (1994). (n.d. not detected/determined)

	Os	Ir	Ru	Rh	Pt	Pd	Au	References
Sulfide fraction Merensky reef	5.2	7.8	35	19	279	120	22	1
Magnesian basaltic suite	n.d.	0.35	3	1.4	17	12	3	2
Reef/melt enrichment factor		22230	11670	13570	16400	10000	7300	
Partition coefficients MORB	n.d.	16400	n.d.	n.d.	2500	35000	18600	3
Experimental sulfide/ silicate partition coefficients	n.d.	35000 $\pm$ 10000	2500 $\pm$ 700	27000 $\pm$ 6000	9000 $\pm$ 6000	34000	1000 $\pm$ 900	4

chemical resorption/thermal erosion features in the anorthositic footwall below the reef. Even the pegmatoidal nature of the reef (e.g., Viljoen and Hieber 1986; Viljoen et al. 1986; Ballhaus and Stumpfl 1986) is consistent with an influx of a new magma: With increasing degree of undercooling (hot magma onto a cooler chamber floor), crystal growth rates pass through a maximum before nucleation rates accelerate (Brandeis et al. 1984; Campbell 1987), with the consequence that a moderately undercooled silicate melt can give rise to pegmatoidal orthocumulates (rapid growth of few crystal nuclei; cf. Ballhaus and Glikson 1989).

If there has been magma addition at the stratigraphic level of the Merensky reef, it is only natural to relate the sulfides and their PGE tenor to that influx of new melt. This, however, is not so straightforward. Relative noble metal abundances in the sulfide fraction of Merensky ore are nearly identical to relative noble metal abundances of the presumed parent melts (Davies and Tredoux 1985; Lee and Tredoux 1986; Fig. 1), implying that the sulfide/silicate partition coefficients (D values) are similar for all noble metals. This is not the case in experimental systems (Tredoux et al. 1995), as Table 1 shows. There are significant discrepancies between the calculated enrichment factors (apparent D values) and the experimental D values (Stone et al. 1990; Bezmen et al. 1990; Peach and Mathez 1994; see also Tredoux et al. 1995). Principally, this would be no problem had the silicate/sulfide mass ratios during mineralisation been small. In such cases, the noble metal spectrum of the exsolving mls would be dominated entirely by the PGE content of the silicate melt, and differences in D values (Table 1) would not matter (as long as the D values are high). The problem, however, is that the exceptional PGE enrichment in the Merensky sulfide melt (500 ppm) requires extremely *high* silicate/sulfide mass ratios, of the order of 10000 to 100000 as Campbell et al. (1983) reasoned. Such mass ratios, however, automatically result in relative PGE abundances in the ore that mimic the magnitudes of the D values; that is, absolute differences in D values should be fully apparent in the chondrite-normalized PGE spectra of the Merensky ore (Fig. 1) which is not the case.

A primary-magmatic mineralisation model also produces several mechanical problems. For example,

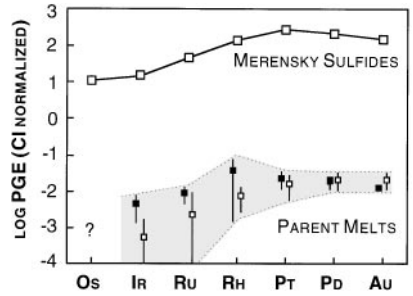

Fig. 1 PGE concentrations in Merensky sulfide ore and potential parent melts to the Bushveld Complex, all normalized to CI chondrite (Anders and Grevesse 1989). Merensky reef data, calculated to 100 percent sulfide, are taken from Naldrett et al. (1987). Possible parent melt compositions (*solid squares* ultramafic sills, *open squares* basaltic suite) are from Davies and Tredoux (1985). Error bars illustrate analytical ranges

silicate/sulfide mass ratios of the order of 10000 to 100000 are only feasible if sulfide unmixing occurs at liquidus temperatures. To allow efficient mechanical concentration, the sulfide droplets should segregate onto the bottom of the magma chamber (i.e., the later ore horizon) at minimal magma viscosities, but the style of mineralisation intuitively expected would be thin massive sulfide stringers close to the base of the Merensky unit rather than sparse disseminated sulfides essentially restricted to the intercumulus spaces. Many structural and textural details are also hard to reconcile with any type of gravity-driven enrichment, be it individual crystals, sulfide droplets, or dense magma "down-spouts" (Naldrett et al. 1986). Ballhaus (1988) noted that the basal orthocumulate pegmatoid occasionally occurs along steeply inclined, even overturned pothole flanks, in roughly the same thickness and appearance as on normal elevation, which cannot be constistent with gravity-driven deposition. Inside the orthocumulate layer there are often thin chromite stringers that are parallel to the large-scale magmatic layering (illustrated by Wagner 1929, p. 117); yet these chromite stringers cut indiscriminately through the earliest cumulus silicates, implying that they could not have had any mechanical support on which to settle at the time of their crystallisation.

It is possible that the noble metals were enriched by fractional crystallization before they became collected

by a sulfide melt (cf. Davies and Tredoux 1985). Indeed, in the southwestern Bushveld, Viljoen and Hieber (1986) noted that the ore grades of the Merensky reef correlate broadly with the thickness of the cumulate piles beneath the reef (supporting the view that the noble metals may relate to the magnesian basalt suite of Davies and Tredoux 1985). The problem though is that the Mg/(Mg + Fe) and Ca/(Ca + Na) ratios of both the Merensky basal orthocumulate and its footwall units are quite primitive, which seems to preclude that the magma had experienced significant fractionation. Many workers (Stumpfl 1974; Boudreau et al. 1986; Stumpfl 1986; Ballhaus and Stumpfl 1986; Mathez 1995) have therefore suggested that the PGE plus Au were concentrated by late- to post-magmatic melts and fluids. However, the chemical and mechanical requirements for these models to work are no less problematic than the mechanics of magmatic mineralisation models (cf. Naldrett et al. 1987). It also remains unanswered why the fluids did not fractionate the noble metals relative to each other during the enrichment process.

The mineralogy of the Merensky ore is probably post-magmatic. A large fraction of the total noble metals forms discrete phases (sulfides, sulfarsenides, Bi-Te-Sn intermetallic compounds, and alloys with Fe; Vermaak and Hendriks 1976). This is likely be a low-temperature phenomenon. At 900° C, the experimentally determined solubilities of Pt, Pd, and Ru (the most abundant PGE in Merensky ore) in pyrrhotite $Fe_{1-x}S$ (the most abundant sulfide phase) exceed the total PGE tenor of the sulfide fraction (500 ppm) by several orders of magnitude (Fig. 2), and the same seems to be true for 500° C (Makovicky et al. 1986). If we accept these experimental data (cf. Ballhaus and Ulmer, in press), then the entire PGE reservoir of the Merensky sulfide fraction is easily accommodated in solid solution, i.e., up to a temperature of 500°C there appears to be no need to nucleate discrete PGE phases. It has been speculated that certain PGE phases (e.g., euhedral laurite RuS_2 grains in chromite) may nucleate directly from silicate melts at magmatic temperatures (Merkle 1992). However, this seems to violate thermochemical principles in that at high temperature, the free energy change of the reaction $Ru + S_2 = RuS_2$ is larger than that of $2Fe + S_2 = 2FeS$ (cf. Barin et al. 1977), with the result that sulfur fugacities (f_{S_2}) to stabilize crystalline RuS_2 are considerably higher than f_{S_2} required to trigger exsolution of a sulfide melt.

This paper quantifies the low-temperature history of the Merensky reef. Its aim is to constrain the temperature at which discrete PGE phases are in stable equilibrium with the BMS. For this purpose, we have analyzed the major BMS of five typical Merensky ore samples for dissolved Pt, Pd, Rh, and Ru using micro-PIXE techniques. The companion paper (Ballhaus and Ulmer, in press) reports new synthesis and reversal experiments to determine the solubilities of Pt and Pd

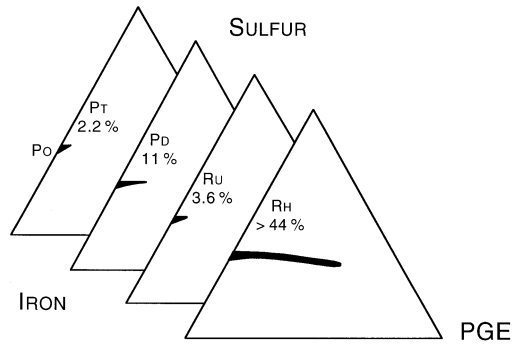

Fig. 2 Experimental PGE solubilities (in weight percent) in pyrrhotite at 900° C (Makovicky et al. 1986). At 500° C, Pt and Ru are reported below detection limit, Pd at 0.5 percent (0.2 percent at 400° C, Makovicky and Karup-Møller 1993), and Rh at 6.7 percent

in synthetic $Fe_{1-x}S$ between 950 and 450°C under controlled f_{S_2}. The major thesis of these papers is that the sulfide-PGE assemblages of the Merensky reef have equilibrated under hydrothermal conditions to exceptionally low temperatures, possibly to below 80 to 90° C. The question of how the noble metals became concentrated in the ore horizon in the first place remains, however, unresolved.

Sample selection

All samples are from Brakspruit shaft, Rustenburg section, southwestern Bushveld Complex (Ballhaus 1988). At Brakspruit, the Merensky reef occurs in a variety of structural settings and mineralogic associations, depicted in Fig. 3. *Normal* Merensky reef is defined as a 25 ± 5 cm thick sulfide-bearing pyroxenitic orthocumulate pegmatoid (e.g., Vermaak 1976; Ballhaus and Stumpfl 1986; Kinloch and Peyerl 1990) that is conformable with the magmatic stratification of the underlying anorthosites. *Pothole* reef occurs where the reef plunges into circular to elliptical depressions in the footwall cumulates, known as potholes (Schmidt 1952; Ballhaus 1988). By definition, pothole reef is cross-cutting to the footwall

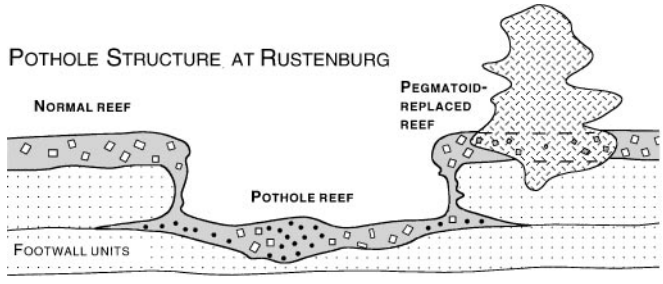

Fig. 3 Schematic section through a pothole to illustrate the types of Merensky reef analysed in this study (thickness of reef greatly exaggerated for clarity). [*Open squares* pyroxenitic reef mostly on normal elevation (samples B20-17 and B20-18) but also in potholes, *filled dots* harzburgitic lens-type reef inside potholes (sample B20-4), *diagonal symbols* replacement pegmatoid intersecting Merensky reef on normal elevation (samples B15-121 and prMR)]. For more information about potholes see Ballhaus (1988) and Kinloch and Peyerl (1990)

Table 2 Sample summary: Sample types analyzed in this study (compare Fig. 3). (*olv* olivine, *opx* orthopyroxene, *cpx* clinopyroxene, *amph* pargasitic amphibole, *cr* chromite, *mt* magnetite, *ilm* ilmenite, *po*1 monoclinic pyrrhotite, *po*2 hexagonal pyrrhotite, *pent* pentlandite, *cpy* chalcopyrite, *cub* cubanite) $\Delta\log f_{S_2}$ is the sulfur fugacity in log-bars relative to the pyrrhotite-pyrite equilibrium. $\Delta\log a_{SiO_2}$ is the silica activity in log-units relative to β-quartz saturation as standard state (650°C and 0.3 GPa)

Topic	Normal reef	Pothole reef	Pegmatoid-Replaced Reef
Sample nos.	B20-17 B20-18	B20-4	B15-121 PRMR
Silicates and oxides	Opx − plag − cpx ± qtz ± cr (feldspathic bronzitite)	Olv − opx − plag − cpx ± cr ± mt (feldspathic harzburgite)	Olv ± amph ± cpx ± ilm (dunite)
Sulfides	Po1 − pent − cpy ± py all intercumulus, dihedral angles $< 60°$	po1 − pent − cpy both intercumulus and droplets in olv	po1 ± po2 (minor pent ± cpy ± cub) droplets, dihedral angles < 60 to $180°$
PGE phases	Sulfides, (sulf)arsenides, intermetallic compounds	Alloys, (sulf)arsenides, sulfides, intermetallic compounds	No PGE minerals observed
Silicate Textures	Orthocumulate	Orthocumulate	Annealed, 120° dihedral angles
$\Delta\log f_{S_2}$	pyrite saturation (0)	− 0.7	− 2.2
$\Delta\log a_{SiO_2}$	quartz saturation (0)	− 0.2 to − 0.25	$<$ − 0.4

cumulates, notably along the flanks of potholes. Pothole reef is more variable in thickness and ranges from significantly thinned contact reef along the pothole flanks to bulky lenses of feldspathic harzburgite orthocumulate pegmatoid in pothole centers. The sample analyzed in this study is from a harzburgitic pothole center. *Pegmatoid-replaced* reef is dunitic to wehrlitic and can be found both on normal elevation and in potholes. It occurs where the ore horizon intersects a replacement pegmatoid (Peyerl 1982; Viljoen and Scoon 1985; Kinloch and Peyerl 1990). These pegmatoids are cross-cutting, rootless, irregular ultramafic bodies and pipes in the critical zone, in which the former magmatic plagioclase-bronzite cumulates were desilicified to olivine-clinopyroxene-amphibole-ilmenite ± sulfide lithologies, possibly by infiltration of a volatile-enriched metasomatic melt or fluid.

Sulfide textures

The mineralogical characteristics of the ore samples are summarized in Table 2. Typical sulfide textures are illustrated in Fig. 4. The sulfide phases in decreasing order of abundance are monoclinic pyrrhotite, pentlandite, chalcopyrite, pyrite, and cubanite, all coexisting with a host of PGE sulfides, sulfarsenides, intermetallic compounds, and alloys (for relative proportions of PGE phases see Vermaak and Hendriks 1976; Kinloch and Peyerl 1990). In pegmatoid-replaced ore, monoclinic pyrrhotite is finely intergrown with a second generation of presumably hexagonal pyrrhotite with a significantly higher metal/sulfure ratio. Exact relative sulfide proportions are difficult to estimate since to our knowledge Fe/Ni ratios of sulfide concentrates of the Merensky reef have not been reported in the literature. We therefore use an Fe/Ni ratio of a bulk sulfide concentrate from the Inziswa layered intrusion (Naldrett 1981) which has Ni/Cu and Pt/Pd ratios quite similar to Merensky ore. Relative proportions then are 53 percent pyrrhotite, 25 percent pentlandite, and 22 percent chalcopyrite. Pyrite is a very minor phase, rarely exceeding one percent. No attempt has been made to characterize the $Fe_{1-x}S$ phases by means of X-ray diffraction, since all sulfides are finely intergrown with each other.

Sulfide compositions

Pyrrhotite, pentlandite, and chalcopyrite were analyzed for major and trace elements using a CAMECA Camebax electron microanalyser (Mainz) and the proton microprobe at CSIRO (North Ryde) using PIXE. The electron probe was calibrated and operated under standard conditions (15 kV accelerating voltage, 20 nA current on the Faraday cup, PAP data reduction). Operation conditions of the proton microprobe are those described by Ryan et al. (1990 a,b). The proton beam diameter is about 20 μm, and penetration depth is up to 70 μm, so the spatial resolution of the proton probe is considerably less than with the electron microprobe. Weighed mean detection limits (MDL) for the trace elements on a 99 percent confidence level are (in ppm): ∼ 15 for Pt, 4 for Pd, 3 for Ru and Rh, 5 for Se, and 70 for Ni. Average sulfide compositions are reported in Table 3. The PGE spectra of the two most important sulfides (monoclinic pyrrhotite and pentlandite) are compared with each other in Fig. 5.

Pyrrhotite

The mole fraction of FeS in monoclinic pyrrhotite ranges from 0.923 in pyroxenitic ore (equilibrium with

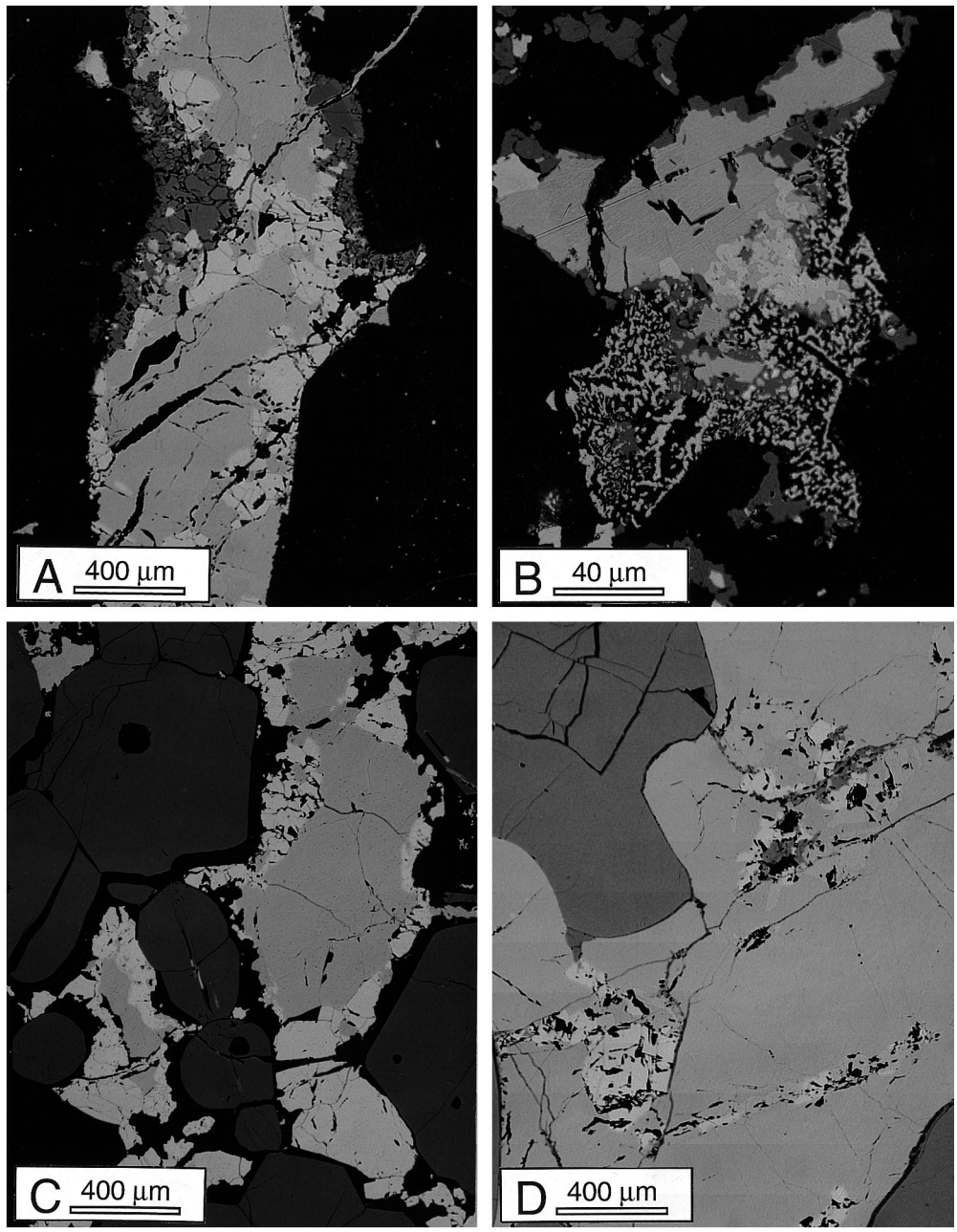

Fig. 4A–D Sulfide textures of the ore samples in reflected light (cf. Table 2): **A** (B20-4) Pyrrhotite (*the main grey mineral*) intergrown with pentlandite (*white*, *with cracks*) and chalcopyrite (*slightly darker grey* than pyrrhotite, several grains attached to pentlandite). Sulfides rimmed by magnetite. The gangue is partly serpentinized olivine. **B** (B20-4) Cooperite (PtS, *light grey*) in myrmekitic intergrowth with pyrrhotite (*grey*), magnetite (*dark grey*), and silicate gangue (*black*). Small white inclusions in cooperite are isoferroplatinum (PtFe). **C** (B20-18) Sulfide aggregates interstitial to subhedral chromite grains (*dark grey*). Pyrrhotite (*grey*) rimmed by pentlandite (*lighter grey*, *with cracks*) and pyrite (*lighter than pentlandite*). Chalcopyrite is slightly darker than pyrrhotite. The dark phase separating sulfide and chromite is silicate gangue, including quartz. **D** (prMR) Pyrrhotite (*grey*) with pentlandite (*white*, *cracks*) and traces of chalcopyrite and bornite (in pentlandite aggregates, *darker than pyrrhotite*). The gangue phase is chromiferous ilmenite

pyrite) to 0.948 in pegmatoid-replaced ore. Hexagonal (?) pyrrhotite in pegmatoid replaced ore has a distinctly higher FeS mole fraction of 0.98. Nickel ranges from 0.7 in monoclinic pyrrhotite coexisting with pyrite, to 0.3 in the harzburgitic sample, and to 0.25 weight percent in pegmatoid-replaced ore. In the FeS-rich hexagonal pyrrhotite of pegmatoid-replaced ore Ni is just above the MDL of the proton probe ($\sim$ 70 ppm). In general, Ni concentrations tend to fall with rising metal/sulfur ratio. Cobalt is below detection limit in all samples even with the proton microprobe.

The only detectable PGE in pyrrhotite is Ru (Rh and Pd are just above MDL), ranging from 45 ± 5 ppm in pyrrhotite coexisting with pyrite, to 34 ppm in pyrrhotite of the harzburgitic sample, and to less than 3 ppm in hexagonal FeS-rich pyrrhotite of pegmatoid-replaced reef. Monoclinic pyrrhotite of pegmatoid-replaced ore has not been analyzed for dissolved PGE because it proved difficult to resolve the two types of pyrrhotite with the proton beam. The Ru correlates positively with both Ni and the metal/sulfur ratio of the $Fe_{1-x}S$ phase (Fig. 6).

Table 3 Average composition of Merensky sulfides. Numbers with digits (in percent) analyzed with electron microprobe, others in ppm with proton microprobe (– below MDL, see text, NA not analyzed, *B20-4* pothole Merensky reef, *B20-17* and *18* pyroxenitic Merensky reef, *B15-121* and *prMR* pegmatoid replaced Merensky reef, *n* number of grains analysed with proton microprobe, *M/S* metal/sulfur ratio on an atomic basis). For typical standard deviations consult figures

Sample no.	*n*	Fe	Ni	Co	Cu	Zn	Ru	Rh	Pd	Se	S	Totals
						Weight percent/ppm						
Monoclinic pyrrhotite												
B-20	6	59.9	0.33	–	0.04	–	34	4	< 4	211	39.7	99.9
B20-17	6	59.2	0.73	–		–	39	6	–	197	40.1	100.0
B20-18	4	59.7	0.62	–	0.04	–	47	< 3	< 3	207	40.4	100.7
B15-121	None	60.6	0.27	–	0.02	–	NA	NA	NA	NA	38.8	99.7
prMR	None	60.7	0.22	–	0.01	–	NA	NA	NA	NA	38.9	99.8
Hexagonal pyrrhotite												
B15-121	1	62.5	< 70	–	–	–	–	–	–	99	36.8	99.3
prMR	5	62.6	167	–	–	–	6	–	–	100	37.2	99.8
Pentlandite												
B20-4	7	30.7	34.4	0.90	–	–	30	99	359	176	33.0	99.1
B20-17	3	30.2	35.6	0.67	93	–	45	26	253	184	33.2	99.6
B20-18	4	30.8	35.7	0.45	0.02	–	42	82	230	185	33.7	100.6
B15-121	4	31.3	27.7	7.53	0.03	–	< 3	< 3	133	78	33.2	99.8
prMR	4	31.7	28.7	5.87	130	–	6	9	114	97	33.4	99.7
Chalcopyrite												
B20M4	4	30.5	0.06	–	33.8	174	–	–	–	126	35.1	99.4
B20-17	3	30.2	0.01	0.03	34.6	304	–	–	–	117	34.9	99.7
B20-18	1	31.0	0.60	0.01	33.4	NA	–	–	–	NA	35.5	100.5
B15-121	None	30.5	0.01	–	34.1	NA	NA	NA	NA	NA	35.1	99.7
prMR	2	30.9	0.01	–	34.5	209	–	–	–	101	35.5	99.6
Cubanite												
B15-121	None	41.3	–	–	22.8	NA	NA	NA	NA	NA	35.7	99.8
prMR	2	41.1	0.07	0.01	22.5	103	–	–	–	110	36.0	99.6

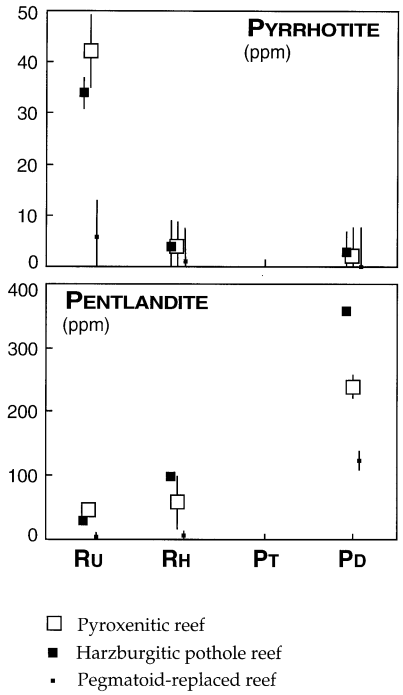

Fig. 5 PGE spectra of pyrrhotite and pentlandite in the Merensky ore. Error *bars* are three weighed standard deviations

Pentlandite

Metal/sulfur ratios of pentlandite are much less variable than in pyrrhotite. When pentlandite coexists with pyrite, it tends to have slightly lower Fe/(Fe + Ni + Co), in accordance with the low temperature Fe–Ni–S phase relations (Craig 1973). In the pyroxenitic and harzburgitic (cumulate-textured) ores, pentlandites are Co-free while in pegmatoid-replaced ore pentlandite contains up to 7 percent Co. Pentlandite is the only base metal sulfide that contains significant PGE; Pd from 114 to 359 ppm, Rh from < 3 to 99 ppm; and Ru from < 3 to 45 ppm. These ranges are in close agreement with those of pentlandites from other magmatic sulfide ores (Cabri et al. 1984, Czamanske et al. 1992), excepting the Pd-rich pentlandites from Stillwater (Cabri et al. 1984). Ru levels in pentlandite do not correlate with the other PGE but vary coherently with Ru, Ni, and metal/sulfur ratio of coexisting pyrrhotite (Fig. 7).

Chalcopyrite

Chalcopyrite is essentially stoichiometric. In pegmatoid-replaced ore chalcopyrite coexists with

Fe	Ni	Co	Cu	S	M/S
		Atomic percent			
46.3	0.24	–	0.03	53.4	0.871
45.6	0.53	–	0.00	53.8	0.857
45.7	0.45	–	0.02	53.8	0.858
47.1	0.20	–	0.01	52.7	0.899
47.2	0.16	–	0.01	52.6	0.900
49.4	0.00	–	0.00	50.6	0.976
49.1	0.00	–	0.00	50.9	0.965
25.2	26.9	0.70	–	47.2	1.117
24.7	27.6	0.52	0.00	47.2	1.119
24.8	27.4	0.35	0.01	47.4	1.110
25.5	21.5	5.81	0.02	47.2	1.119
25.8	22.2	4.53	0.00	47.4	1.109
25.1	0.05	0.00	24.4	50.4	0.985
24.9	0.01	0.02	25.0	50.0	0.999
25.2	0.46	0.01	23.9	50.4	0.985
25.1	0.00	0.00	24.6	50.2	0.990
25.1	0.01	0.00	24.7	50.2	0.991
33.4	0.0	0.00	16.2	50.3	0.987
33.2	0.1	0.00	16.0	50.7	0.971

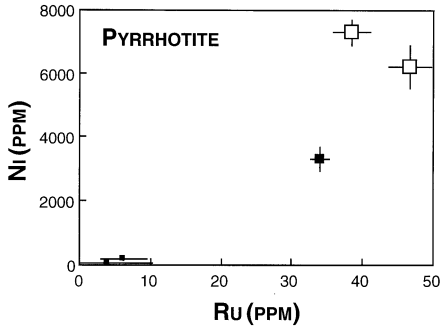

Fig. 6 Ni and Ru in pyrrhotite. Ni in pyrrhotite in pegmatoid-replaced ore has been analysed with proton microprobe. Errors *bars* are three weighed standard deviations. Symbols as in Fig. 5

cubanite. The only trace elements observed in chalcopyrite in significant quantities are Se and Zn. Neither chalcopyrite nor cubanite accommodate any PGE in detectable quantities, in accordance with findings of Czamanske et al. (1992).

Are the sulfides PGE-saturated ?

We may now calculate whether and by how much the sulfides of the Merensky ore are oversaturated with

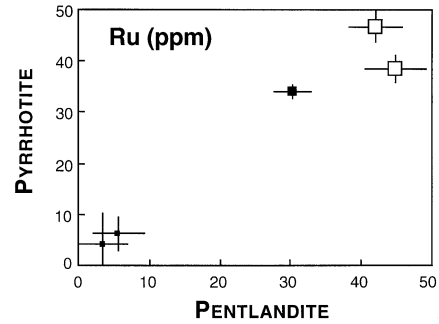

Fig. 7 Ru in coexisting pyrrhotite and pentlandite. Error bars are three weighed standard deviations. Symbols as in Fig. 5

respect to individual PGE at the temperature of final equilibration. We assume that the PGE plus Au content in the sulfide fraction is 500 ppm, and that the noble metals occur in the proportions as shown in Table 1. As deduced above, modal proportions of sulfide phases are assumed to be 53 percent pyrrhotite, 23 percent pentlandite, and 22 percent chalcopyrite (ignoring minor phases). Even if this modal estimate is out in absolute terms by 10 percent (since it is based on Fe/Ni ratios of sulfide concentrates from another layered intrusion), this will have no profound influence on the saturation argument presented below.

With respect to Pt, the Merensky ore must be many times oversaturated. None of the sulfides contain any detectable Pt, so virtually the entire Pt tenor of the Merensky sulfide fraction must reside in discrete PGE phases. With regard to Pd the sulfides are also oversaturated, albeit at a lower level. If the average Pd content in pentlandites of the pyroxenitic ore is taken to be 250 ppm, and if it is accepted that pyrrhotite is Pd-free, then the sulfide fraction is oversaturated with respect to Pd by about a factor of two. In the normal Merensky reef, the most common Pd-bearing minerals that coexist with BMS are braggite (*Pt*, Pd, Ni)S followed by Pd-Pt bismuthotellurides (Vermaak and Hendriks 1976; Kinloch 1982). Palladium-rich vysotskite (*Pd*, Pt, Ni)S (common in the Pd-rich J-M reef of the Stillwater Complex; Naldrett et al. 1987) is not reported. We suggest that total Pd contents, Pd/Pt bulk ratios, and sulfur fugacities (cf. Barin et al. 1977) were too low to stabilize vysotskite.

For Ru, the mass balance result is not quite so clear. Ruthenium enjoys a much larger reservoir in Merensky ore since it dissolves to approximately the same quantities in both pyrrhotite and pentlandite. If we assume the average Ru in these phases to be 40 ppm and accept the Ru tenor of the sulfides of 40 ppm Ru (Table 1), both pyrrhotite and pentlandite should be oversaturated with respect to Ru by a factor of about 1.25. This number is probably within the error of our calculation. The observation that Ru concentrations are about the same in pyrrhotite and pentlandite argues against saturation of the sulfides with Ru, unless the

activity coefficients for Ru in pyrrhotite and pentlandite happen to be the same. On the other hand, laurite (RuS_2) is reported from all types of Merensky reef (Kinloch and Peyerl 1990), suggesting that the sulfides must have become saturated at some point with respect to Ru.

With respect to Rh, we believe that the sulfides are undersaturated. If we assume the average Rh in pentlandite of pyroxenitic reef to be 60 ppm and Rh in the bulk sulfide to be 15 ppm, Rh-rich phases are unlikely to be stable. It is no surprise then, that discrete Rh-enriched PGE phases such as hollingworthite (Rh, Pt, Pd, Ir, Ru)AsS (Stumpfl 1972) are rare indeed in Merensky ore (Vermaak and Hendriks 1976).

Equilibration history of Merensky ore

If the sulfides are PGE undersaturated at 500°C as experiments (Makovicky et al. 1986) suggest, why and at what temperatures did discrete PGE minerals form in the Merensky reef?

One important factor was probably the presence of minor components in the magmatic mls with chemical affinities to PGE (As, Sb, Bi, Te, Sn), which may have stabilized discrete PGE phases relative to PGE in solid solution (cf. Fleet et al. 1993). The PGE compounds with these elements indeed constitute a significant fraction of the PGE mineral spectrum reported from Merensky ore (Kinloch and Peyerl 1990). Equally important, however, could have been the down-temperature equilibration history of the Merensky reef. Below, we argue that the BMS have continued to exsolve trace metals to temperatures well below the lowest experimental temperatures at which PGE solubility in BMS has been studied.

Equilibration temperatures of metal/sulfur ratios

The mole fraction of FeS in pyrrhotite permits calculation of both f_{S_2} and temperature of equilibration of the metal/sulfur ratio. Sulfur fugacities can be calculated relative to the pyrite-pyrrhotite equilibrium if we combine Toulmin and Barton's (1964) equation for absolute sulfur fugacities with a polynomial fit through their pyrite-pyrrhotite-f_{S_2} data:

$$\Delta\log f_{S_2} = (70 - 85.83\,X_{FeS}) * (1000/T - 1) + 39.3 * (1 - 0.9981 * X_{FeS})^{0.5} + 29.9 - 0.0692 * T + 0.0000269 * T^2 \quad (1).$$

In this equation, $\Delta\log f_{S_2}$ is the relative sulfur fugacity (f_{S_2}) given in log-bars relative to pyrite saturation, X_{FeS} is the mole fraction of FeS in the $Fe_{1-x}S$ phase, and T is the temperature in K. Equation (1) is valid above 573 K because below that temperature the pyrite-pyrrhotite solvus reverses its slope (Craig and Scott 1976).

Temperature and relative f_{S_2} pairs can be obtained with Eq. (1) if pyrrhotite coexists with pyrite. The mole fraction of FeS in the $Fe_{1-x}S$ phase in equilibrium with pyrite increases with falling temperature (Toulmin and Barton 1964) because the enthalpy change of the reaction $2Fe + S_2 = 2FeS$ is smaller than that of $2FeS + S_2 = FeS_2$ (cf. Johnson et al. 1992). A temperature is obtained if one varies the temperature input in Eq. (1) until calculated and expected relative f_{S_2} values (pyrite saturation) converge at zero. For the two pyrite-saturated pyroxenitic normal reef samples B20-17 and B20-18 ($\Delta\log f_{S_2} = 0$), calculated and predicted relative f_{S_2} converge at a temperature of 560 ± 5°C. For the harzburgitic ore sample B20-4 we calculate a relative f_{S_2} of -0.7 log-bars at that temperature. For the two pegmatoid-replaced Merensky ore samples (B15-121 and prMR), we calculate relative f_{S_2} values of around -2.2 log-bars (cf. Table 2). Note that the latter value may be a maximum, since the main $Fe_{1-x}S$ phase (monoclinic pyrrhotite?) has exsolved a second $Fe_{1-x}S$ phase (hexagonal pyrrhotite?) with a higher metal/sulfur ratio that has not been re-integrated.

Relationship between f_{S_2}, metal/sulfur ratios, and silica activity

In absolute terms, the temperature of 560 ± 5°C calculated for the pyrite-bearing sample must be an arbitrary value along the down-temperature equilibration path of the samples, since the sulfides have continued to reset below that temperature. However, the absolute differences in relative f_{S_2} among the ore types, recorded at that arbitrary temperature, still are relevant. We argue that they record the approximate range in relative f_{S_2} at the solidus temperatures of these ore samples. The reason for this argument is that relative f_{S_2} correlates with silica activities at which these samples have solidified, as specified below.

In natural iron-bearing silicate-sulfide systems, f_{S_2}, f_{O_2}, and the activity of silica (a_{SiO_2}) cannot vary independently (cf. Haughton et al. 1974). This can be illustrated by the endmember equilibria

$$Fe_2SiO_{4\ olivine} + SiO_2 = 2FeSiO_{3\ opx} \quad (2)$$

$$3Fe_2SiO_{4\ olivine} + O_2 = 2Fe_3O_{4\ spinel} + 3SiO_2 \quad (3)$$

$$6FeS_{\ pyrrhotite} + 4O_2 = 2Fe_3O_{4\ spinel} + 3S_2 \quad (4)$$

For example, if silica becomes enriched during differentiation (e.g., by olivine fractionation; Eq. 2), f_{O_2} will rise (Eq. 3), and this will progressively oxidize the FeS

component in pyrrhotite until pyrite saturation occurs (Eq. 4). The parameter with the greatest influence on the system will be a_{SiO_2}, because silicates (or silica species in the melt) are more abundant than any phase or component that could buffer f_{S_2} or f_{O_2}. Consequently, if relative f_{S_2} is to be imposed by a_{SiO_2}, the stoichiometric coefficients of eqn (2) to (4) predict that a range in relative f_{S_2} of 2.2 log-bars (Table 2) should correspond to a range in a_{SiO_2} of 0.54 log-units relative to β-quartz saturation.

This requirement is indeed closely met (a_{SiO_2} values given below are for 650° C and 0.3 GPa, calculated with the software package of Johnson et al. 1992):

1. *Harzburgitic ore* is the earliest reef facies and formed when the magma had reached a silica activity consistent with orthopyroxene saturation. Consequently, a_{SiO_2} may be calculated with the equilibrium Mg_2SiO_4 (olivine) + $SiO_2 = 2MgSiO_3$ (orthopyroxene), for which we calculate an a_{SiO_2} range of -0.20 to $-0.25 \log_{10}$ units relative to β-quartz saturation. The Mg/(Mg + Fe) ratios in olivine and orthopyroxene are around 0.8 (Ballhaus et al. 1988), and solution models are from O'Neill and Wall (1987). The calculated f_{S_2} is $-0.7 \log_{10}$ bars relative to pyrite saturation, not quite the four orders difference to relative a_{SiO_2} demanded by stoichiometry but reasonably close.
2. *Pyroxenitic ore* formed when quartz saturation had occurred in the interstitial melt of the Merensky orthocumulate. The presence of free quartz constrains $\log_{10} a_{SiO_2}$ to zero. The presence of pyrite defines relative f_{S_2}, as defined by Eq. (1), also to zero.
3. *Pegmatoid-replaced ore* is thought to have formed by back-reaction of higher temperature (pyroxenitic or harzburgitic) reef with volatile-rich, low a_{SiO_2} intercumulus melts that may have segregated from adjacent magmatic cumulates. In replacement pegmatoids, plagioclase is unstable and converts, prior to complete resorption, to pure anorthite (cf. Schiffries 1982). The Al_2O_3 content in clinopyroxene is around 2 to 3 percent (C. Ballhaus, unpublished data). This places the upper limit of a_{SiO_2} to below the equilibrium $CaAl_2SiO_6$ (clinopyroxene) + $SiO_2 = CaAl_2Si_2O_8$ (plagioclase) for which we obtain an a_{SiO_2} of around -0.5 to $-0.6 \log_{10}$ units relative to β-quartz saturation (CaTs solution model of Herzberg 1978). The maximum relative f_{S_2} is -2.2 log-bars.

Obviously, the range in a_{SiO_2} among the three types of ore (~ 0.5–0.6 log-units) matches reasonably closely the range in relative f_{S_2} (~ 2.2 log-bars), as demanded by the 1 : 4 stoichiometry of the equilibria (2) to (4). This suggests that the differences in relative f_{S_2} we calculate with Eq. (1) may still record the metal/sulfide ratios of the bulk sulfide at the time and temperature the silicate equilibria closed with respect to a_{SiO_2}. The implication is that, with respect to sulfur, the Merensky reef may have behaved as a closed system since the late-magmatic stage.

Subsolidus cooling history

The coexistence of pyrite, pyrrhotite, and pentlandite in pyroxenitic ore defines the only point along the down-temperature path that may be constrained reasonably well. Craig (1973) reports that pyrite and pentlandite coexist below 213 ± 12°C, while Misra and Fleet (1973) argue that the assemblage should be stable below 280° C. All Merensky ore samples have equilibrated through at least this temperature window. The absence of pyrite in harzburgitic and pegmatoid-replaced ore only indicates that f_{S_2} and a_{SiO_2} were too low to sustain pyrite, as corroborated by our relative f_{S_2} and a_{SiO_2} calculations in Table 2.

The most promising approach to quantify sulfide closure temperatures may be the Ni content of pyrrhotite in equilibrium with pentlandite. Misra and Fleet (1973) found that mss breaks down below 400° C at a composition of about 33 atomic percent Ni. At 300° C the pyrrhotite-pentlandite solvus is at 25, and at 230° C at 17 atomic percent Ni (Misra and Fleet 1973). Natural pyrrhotites rarely contain Ni > 1 atomic percent (cf. data compilation of Misra and Fleet 1973), and those of the Merensky reef are no exception (Table 3). Let us assume the temperature slope of the pyrrhotite-pentlandite solvus stays approximately the same down to the closure temperatures of natural pyrrhotite-pentlandite pairs; if we then extrapolate Misra and Fleet's data down-temperature, the Merensky pyrrhotites may have continued to exsolve their Ni and their dissolved PGE down to temperatures < 80 to 90° C. Experiments described in Ballhaus and Ulmer (in press) provide independent support that such exceptionally low closure temperatures for magmatic ores are indeed realistic.

Summary and conclusions

1. We have determined PGE levels in solid solution in BMS by proton microprobe using PIXE. Like in many other magmatic ores, PGE levels are mostly at the mean detection limit of the proton microprobe which varies for individual PGE between 3 and 15 ppm. Pentlandite is the only phase that accommodates appreciable PGE, notably Pd.
2. We present a mass balance calculation to test whether and by how much the sulfide fraction of Merensky ore is oversaturated with PGE at the present state of equilibration. With respect to Pt, we note that the sulfides must be several times oversaturated; virtually the entire Pt reservoir of the ore occurs in the form of discrete PGE minerals. With regard to Pd, the sulfides appear to be oversaturated by about a factor of two. Ru is possibly just above the saturation levels of the sulfides as the frequent presence of laurite supports, while with respect to Rh the sulfides are undersaturated.

3. If the sulfides of the Merensky reef are undersaturated with PGE at 500° C, discrete PGE phases coexisting with BMS must be a low temperature phenomenon. The observation that calculated f_{S_2} ranges vary coherently with ranges in calculated a_{SiO_2} suggests that the reef may have behaved as a closed system with respect to S since the late-magmatic stage. The implication is that metal/sulfur bulk ratios may have been left unchanged since the late intercumulus state of the ores, which we tentatively place near 650° C.
4. All ore assemblages have equilibrated (under largely isochemical conditions ?) below the maximum stability of pentlandite with pyrite, which is reported below 280 (Misra and Fleet 1973) and 213 $\pm$ 12° C (Craig 1973). The final closure temperatures of the sulfides are even lower and are approximated with the pentlandite-pyrrhotite solvus. At the solvus, the Ni content in pyrrhotite decreases from $\sim$ 33 at $<$ 400° C, to 25 at 300° C, and to around 17 atomic percent at 230° C (Misra and Fleet 1973). If we extrapolate that temperature effect down-temperature, the pyrrhotites in natural Merensky ore may have continued to exsolve Ni, and by implication their dissolved PGE, to temperatures $<$ 80 to 90° C.

Acknowledgments We thank Gary Suter for keeping the CSIRO proton microprobe in excellent running order at all times. We also thank Gregor Markl, Klaus Mezger, Eugen Stumpfl, and Roland Stalder for their comments on the submitted version. The final manuscript has benefitted greatly from a thorough and insightful review by Marian Tredoux, and comments by an anonymous referee. Chris Ballhaus acknowledges generous financial support by the Heisenberg Referat of the DFG.

References

Anders E, Grevesse N (1989) Abundances of the elements: meteoritic and solar. Geochim Cosmochim Acta 53:197–214

Ballhaus C (1988) Potholes of the Merensky reef at Brakspruit shaft, Rustenburg Platinum Mines: primary disturbances in the magmatic stratigraphy. Econ Geol 83:1140–1158

Ballhaus C (1995) Is the upper mantle metal-saturated? Earth Planet Sci Lett 132:75–86

Ballhaus C, Stumpfl EF (1986) Sulfide and platinum mineralisation in the Merensky reef: evidence from hydrous silicates and fluid inclusions. Contrib Mineral Petrol 94:193–204

Ballhaus C, Glikson AY (1989) Magma mixing and intraplutonic quenching in the Wingellina Hills intrusion, Giles Complex, central Australia. J Petrol 30:1443–1469

Ballhaus C, Cornelius M, Stumpfl EF (1988) The upper critical zone of the Bushveld Complex and the origin of Merensky-type ore horizon – a discussion. Econ Geol 83:1082–1091

Ballhaus C, Ulmer P (1996) Platinum-group elements in the Merensky reef. II. Experimental solubilities of Pt and Pd in synthetic $Fe_{1-x}S$ between 950 and 450° C under controlled f_{S_2} and f_{H_2}. Geochim Cosmochim Acta (in press)

Barin I, Knacke O, Kubaschewski O (1977) Thermochemical properties of inorganic substances. Springer Verlag, Heidelberg New York, Berlin

Bezmen NL, Asif M, Brügmann GE, Romanenko IM, Naldrett AJ (1994) Distribution of Pd, Rh, Ru, Ir, Os, and Au between sulfide and silicate melts. Geochim Cosmochim Acta 58:1251–1260

Boudreau AE, Mathez EA, McCallum IS (1986) Halogen geochemistry of the Stillwater and Bushveld Complexes: evidence for transport of the platinum-group elements by chloride-rich fluids. J Petrol 27:967–986

Brandeis G, Jaupart C, Allègre CJ (1984) Nucleation, crystal growth and the thermal regime of cooling magmas. J Geophys Res 89:10161–10177

Cabri LJ, Blank H, Laflamme JHG, Nobiling R, Sizgoric MB, Traxel K (1984) Quantitative trace element analyses of sulfides from Sudbury and Stillwater by proton microprobe. Can Mineral 22:521–542

Campbell IH (1987) Distribution of orthocumulate textures in the Jimberlana intrusion. J Geol 95:35–54

Campbell IH, Naldrett AJ, Barnes SJ (1983) A model for the origin of platinum-rich sulfide horizons in the Bushveld and Stillwater complexes. J Petrol 24:133–165

Craig JR (1973) Pyrite-pentlandite assemblages and other low-temperature relations in the Fe–Ni–S system. Am J Sci 273-A: 496–510

Craig JR, Scott SD (1976) Sulfide phase equilibria. In: Ribbe PH (ed) Sulfide mineralogy. (Reviews in mineralogy 1) Mineral Soc Am, Washington, DC, pp CS1–CS 110

Czamanske GK, Kunilov VE, Zientek ML, Cabri LJ, Likhachev AP, Calk LC, Oscarson RL (1992) A proton-microprobe study of magmatic sulfide ores from the Noril'sk-Talnakh district, Siberia. Can Mineral 30:249–288

Davies G, Tredoux M (1985) The platinum-group element and gold contents of marginal rocks and sills of the Bushveld Complex. Econ Geol 80:838–848

Fleet ME, Chryssoulis SL, Stone WE, Weisener CG (1993) Partitioning of platinum-group elements and Au in the Fe–Ni–Cu–S system: experiments on the fractional crystallization of sulfide melt. Contrib Mineral Petrol 115:36–44

Haughton DR, Roeder PL, Skinner BJ (1974) Solubility of sulfur in mafic magmas. Econ Geol 69:451–467

Herzberg CT (1978) Pyroxene geothermometry and geobarometry: experimental and thermodynamic evaluation of some subsolidus phase relations involving pyroxenes in the system $CaO - MgO - Al_2O_3 - SiO_2$. Geochim Cosmochim Acta 92: 945–957

Johnson JW, Oelkers EH, Helgeson HC (1992) SUPCRT92: a software package for calculating the standard molal thermodynamic properties of minerals, gases, aqueous species, and reactions from 1 to 5000 bars and 0 to 1000° C Comput Geosci 18:899–947

Kinloch ED (1982) Regional trends in the platinum-group mineralogy of the critical zone of the Bushveld Complex, South Africa. Econ Geol 77:1328–1347

Kinloch ED, Peyerl W (1990) Platinum-group minerals in various rock types of the Merensky reef: genetic implications. Econ Geol 85:537–555

Kruger J, Marsh (1982) Significance of $^{87}Sr/^{86}Sr$ ratios in the Merensky cyclic unit of the Bushveld Complex. Nature 298: 53–55

Lee C, Tredoux M (1986) Platinum-group element abundances in the lower and lower critical zone of the eastern Bushveld Complex. Econ Geol 81:1087–1095

Makovicky E, Karup-Møller S (1993) The system Pd–Fe–S at 900°, 725°, 550°, and 400° C. Econ Geol 88:1269–1278

Makovicky M, Makovicky E, Rose-Hansen J (1986) Experimental studies on the solubility and distribution of platinum-group elements in base metal sulphides in platinum deposits. In: Gallagher MJ, Ixer RA, Neary CR, Prichard HM (eds) Metallogeny of basic and ultrabasic rocks. Inst Min Metall London, pp 415–425

Mathez EA (1995) Magmatic metasomatism and formation of the Merensky reef, Bushveld Complex. Contrib Mineral Petrol 119:277–286

Merkle RKW (1992) Platinum-group minerals in the middle group of chromitite layers at Marikana, western Bushveld Complex: indication for collection mechanisms and postmagmatic modifications. Can J Earth Sci 29:209–221

Misra KC, Fleet ME (1973) The chemical compositions of synthetic and natural pentlandite assemblages. Econ Geol 68:518–539
Naldrett AJ (1981) Nickel sulfide deposits: classification, composition, and genesis. Econ Geol 75th Anniv Vol 1981:628–685
Naldrett AJ, Gasparrini EC, Barnes SJ, Von Gruenewaldt G, Sharpe MR (1986) The upper critical zone of the Bushveld Complex and a model for the origin of Merensky-type ores. Econ Geol 81: 1105–1117
Naldrett AJ, Cameron G, Von Gruenewaldt G, Sharpe MR (1987) The formation stratiform PGE deposits in layered intrusions. In: Parsons I (ed) Origins of igneous layering. D Reidel Publ Co, Dordrecht, pp 313–397
O'Neill HStC, Wall VJ (1987) The olivine-orthopyroxene-spinel oxygen geobarometer, the nickel precipitation curve, and the oxygen fugacity of the Earth's upper mantle. J Petrol 28: 1169–1191
Peach CL, Mathez EA (1994) Constraints on the formation of platinum-group element deposits in igneous rocks. EOS Suppl Am Geophys Union Fall Meet 710
Peach CL, Mathez EA, Keays RR (1990) Sulfide melt-silicate melt distribution coefficients for noble metals and other chalcophile elements as deduced from MORB: implications for partial melting. Geochim Cosmochim Acta 54:3379–3389
Peach CL, Mathez EA, Keays RR, Reeves SJ (1994) Experimentally determinated sulfide melt-silicate melt partition coefficients for iridium and palladium. Chem Geol 17:361–377
Peyerl W (1982) The influence of the Driekop dunite pipe on the platinum-group mineralogy of the UG-2 chromitite in its vicinity. Econ Geol 77:1432–1438
Ryan CG, Cousens DR, Sie SH, Griffin WL (1990a) Quantitative analysis of PIXE spectra in geoscience applications. Nucl Instrum Methods Phys Res B49:271–276
Ryan CG, Cousens DR, Sie SH, Griffin WL, Suter G, Clayton E (1990b) Quantitative PIXE microanalysis of geological materials using the CSIRO proton microprobe. Nucl Instrum Methods Phys Res B47:55–71
Schiffries CM (1982) The petrogenesis of a platiniferous dunite pipe in the Bushveld Complex: infiltration metasomatism by a chloride solution. Econ Geol 77:1439–1453
Schmidt ER (1952) The structure and composition of the Merensky reef and associated rocks in the Rustenburg platinum mine. Trans Geol Soc S A fr 55:234–279
Stone WE, Crocket JH, Fleet ME (1990) Partitioning of palladium, iridium, and gold between sulfide liquid and basalt melt at 1200° C. Geochim Cosmochim Acta 54:2341–2344
Stumpfl EF (1972) Compositional variation in the hollingworthite-irarsite group. Nuclear Jahrb Mineral Monatsh 9: 406–415
Stumpfl EF (1974) The genesis of platinum deposits: further thoughts. Min Sci Eng 6:120–141
Stumpfl EF (1986) Distribution, transport and concentration of platinum-group elements. In: Gallagher MJ, Ixer RA, Neary CR, Prichard HM (eds) Metallogeny of basic and ultrabasic rocks. Inst Min Metall London, pp 379–394
Toulmin P, Barton PB (1964) A thermodynamic study of pyrite and pyrrhotite. Geochim Cosmochim Acta 28:641–671
Tredoux M, Lindsay NM, Davies G, McDonald I (1995) The fractionation of platinum-group elements in magmatic systems, with the suggestion of a novel causal mechanism. S Afr J Geol 98:157–167
Vermaak CF (1976) The Merensky reef—thoughts on its environment and genesis. Econ Geol 71:1270–1298
Vermaak CF, Hendriks LP (1976) A review of the mineralogy of the Merensky reef, with specific reference to new data on the precious metal mineralogy. Econ Geol 71:1244–1269
Viljoen MJ, Scoon RN (1985) The distribution and main geologic features of discordant bodies of iron-rich ultramafic pegmatite in the Bushveld Complex. Econ Geol 80:1109–1128
Viljoen MJ, Hieber R (1986) The Rustenburg section of Rustenburg Platinum Mines Limited, with reference to the Merensky reef. In: Anhaeusser CR, Maske S (eds) Mineral deposits of southern Africa. Geol Soc S Afr, Johannesburg pp 1107–1134
Viljoen MJ, De Klerk WJ, Coetzer PM, Hatch NP, Kinloch E, Peyerl W (1986) The Union section of Rustenburg Platinum Mines Limited, with reference to the Merensky reef. In: Anhaeusser CR, Maske S (eds) Mineral deposits of southern Africa. Geol Soc S Afr, Johannesburg, pp 1061–1090
Wagner PA (1929) The platinum deposits and mines of South Africa. Oliver and Boyd, Edinburgh